LHCb 2003-012, VELO
February, 2003
DRAFT 3.00

R-Sensor sectors and Strip Pitch

authors
Leo Wiggers, Marko Zupan
NIKHEF, Amsterdam, The Netherlands
Paula Collins, Hans Dijkstra, Doris Eckstein, Thomas Ruf
CERN, Geneva, Switzerland
Chris Parkes
University of Glasgow, Glasgow, Scotland, UK
Ivan Kisel
Kirchhoff-Institut fur Physik, Ruprecht-Karls-Universitat Heidelberg, Germany
Mariusz Witek
Krakow, Poland
Olivier Callot
Laboratoire de l'Accélérateur Linéaire (LAL), Orsay, France

Abstract

Four different designs for the layout of the R-sensors of the VELO are compared for their performance in signal to noise (S/N), the Pile-up Veto, the L1-tracking, the off-line tracking and the impact parameter resolution. The design as presented in the VELO-TDR was optimised solely for the impact parameter resolution, but a design where all R-strips cover a 45° sector, rather than strips at larger radii covering 90° sectors, is favoured for the expected S/N, the reconstruction time, and the number of ghost tracks, while the loss in impact parameter resolution is small. Hence it is proposed to change to a new design, with 45° sectors, and a variable strip pitch keeping the same number of channels per sensors as proposed in the VELO-TDR.

1 Introduction

The proposed R-sensor layout in the VELO-TDR [1] covers 182° degrees in ϕ for radii between 8 and 42 mm. The strip layout consisted of subdividing the strips at radii below 24.1 mm in four sectors of approximately 45° while for larger radii the strips are only subdivided in two sectors covering 91° degrees each. The aim was to save channels at larger radii, where the occupancy is low, and use these channels to decrease as much as possible the pitch, especially at small radii to improve the impact parameter resolution. The resulting strip pitch as a function of radius is shown as 'TDR' in Fig. 1. A design with subdividing the strips in four sectors at all radii has advantages for the uniformity of the capacitance per channel, the execution time of the track reconstruction, and the number of clone and ghost tracks. Since the number of channels per sensor cannot be increased beyond 2048 for practical reasons, the strip pitch needs to be increased to cover the same area with four sectors at all radii. The three pitch proposals considered are

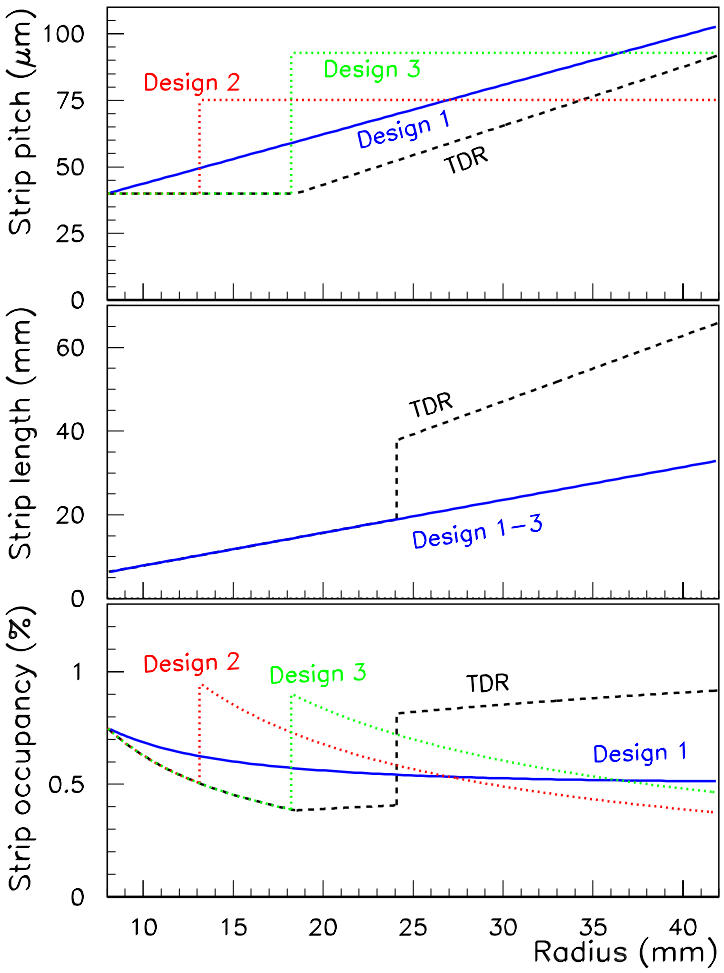

Figure 1: The strip pitch as a function of the radius of the different R-sensor strip designs.

shown in Fig. 1 as designs 1,2 and 3. The relations between pitch and radius for the different designs are:

TDR The TDR design, four(two) sectors for radii below(above) 24.1 mm, and the strip pitch is 40μm for radii below 18.5 mm, while for radii (r) larger than 18.5 mm the pitch is 40+(r-18.5)$\times$(92-40)/(42-18.5) μm, with the radius r in mm.

1 The strip pitch is 40+(103-40)$\times$(r-8)/(42-8) μm.

2 The strip pitch is 40μm at radii smaller than 13.12 mm, and 75.2 μm at larger radii.

3 The strip pitch is 40μm at radii smaller than 18.24 mm, and 92.8 μm at larger radii.

For all performance studies SICB v248r4 and Brunel v14r0 have been used, with modified VELO Detector elements for the different layouts. This note is organised as follows, in the next section the consequences for the S/N and the additional dead area introduced by having to add bias resistors are discussed, in section 3 the performance of the Pile-up Veto is shown for the designs proposed. Section 4 and 5 deals with the

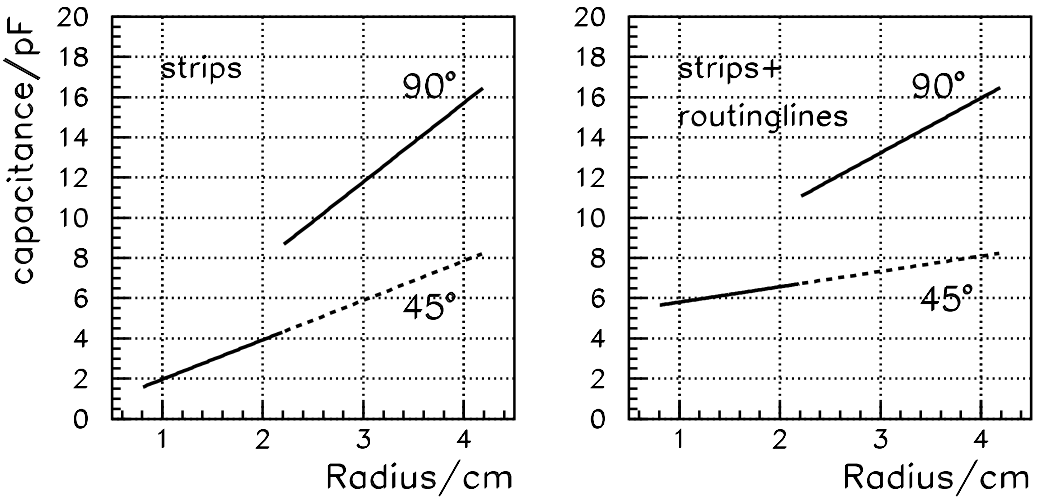

Figure 2: The capacitance as a function of radius introduced by the strip lines (left) and by the strip lines together with the routing lines (right) for the old and new layout.

tracking for the Level-1 trigger and off-line respectively. Section 6 presents the expected degradation in physics performance using the impact parameter as a measure. The last section summarises the findings, and draws the conclusion.

2 Sensor layout, S/N and coverage

A study of the noise of a Micron PR03 R-measuring detector was performed in order to estimate the changes in noise and signal to noise due to the new design with 45° sectors. The data used were collected in Autumn 2001 in a test-beam at the CERN SPS. The sensor is of n-on-n type with a thickness of 200μm and its geometry identical to the PR02 R-detector desribed in [4]. The detector was equipped with three 6-SCTA128A hybrids carrying 16 chips. In the data sample analysed 10 chips were read out.

The noise after subtraction of common mode and pedestals was assumed to consist of a constant term and a term depending on the capacitance C_i at the chip input, i.e. Noise=540 e^-+70 e^- $\times$ C_i for the SCTA128A. The capacitive load introduced was expressed as $C_i = a \times SL_i + b \times RL_i + c \times FL_i$, where SL_i is the length of a strip, RL_i is the length of its routing line and FL_i is the length of its fan-in line. A fit to the noise as a function of strip number results in values for a, b and c, which quantify the relative contributions to the noise and allow a prediction of the noise when using 45° sectors. The method and its uncertainties will be described in more detail in a subsequent note.

The contribution of the strips and routing lines to the detector capacitance is illustrated in Fig. 2 for a = 2.5 pF/cm and b = 1.2 pF/cm. For the tested detector a big variation in capacitance is observed between the 45° sectors at inner radii and the 90° sectors at outer radii (solid line). Reducing the strip length by a factor of two reduces

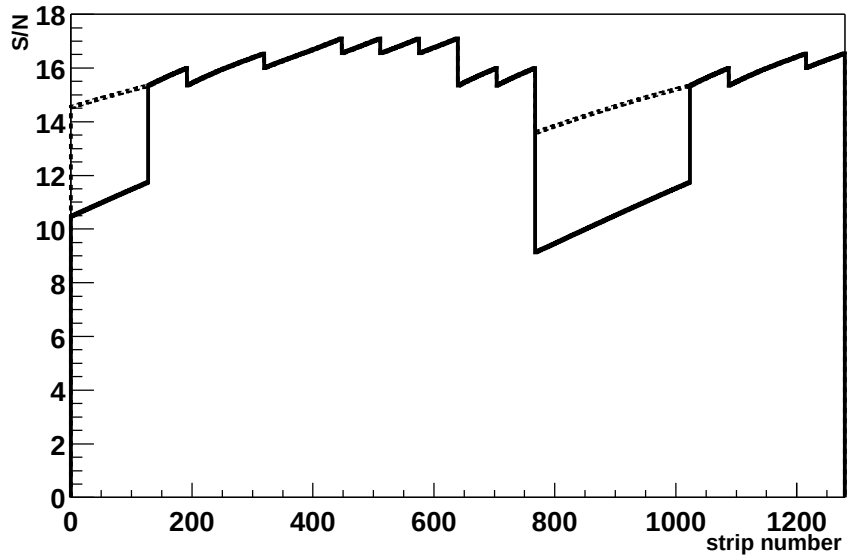

Figure 3: S/N as function of strip number in the PR03 R-measuring detector as used in the test-beam (solid line) and prediction of the S/N assuming 45° sectors (dashed line).

the strip capacitance by the same amount and leads to a much smaller variation over the sensor (45° line). The signal to noise (S/N) ratio predicted using the result of the noise fit and subtracting the contribution of the fan-in is shown in Fig. 3 for the 90° layout used (solid line). The drop in S/N seen for strips below 128 and between 768 and 1023 is due to the increased strip length in the 90° parts. An increase of the signal to noise ratio of 20% to 40% can be expected by reducing the strip length by a factor of two, shown by the dashed lines in Fig. 3.

For this test-beam example the change of detector geometry going to 45° strips shows a clear advantage, as all strips then show a similar and acceptable S/N.

A design with 45° sectors at all radii will extend the inefficient area due to the bias rail for the two sectors in the centre of the detector. This bias rail might run down the centre of the detector, biasing strips to either side, or there might be an individual bias rail for each 45° sector. In the worst case scenario, this leads to a completely inefficient region of 55 μm between the ends of the diodes. In this case the inefficiency increases from 0.084% for the TDR design to 0.11% or 0.21% for the 45° design, assuming a 1/r**2 distribution of tracks. The inefficiency in the overlap region remains unchanged. In reality there is some efficiency from the bias rail region, in particular from inclined tracks. This efficiency can be recovered in the offline to a large extent by combining signals from abutting strips, as has been shown [2]. These clusters are of particular interest for the alignment.

3 Effect of the 45° sector design for the Pile-up Veto

In the following, three designs are compared:

TDR the TDR layout, combining 45° sectors at the smaller radii to 90° sectors.

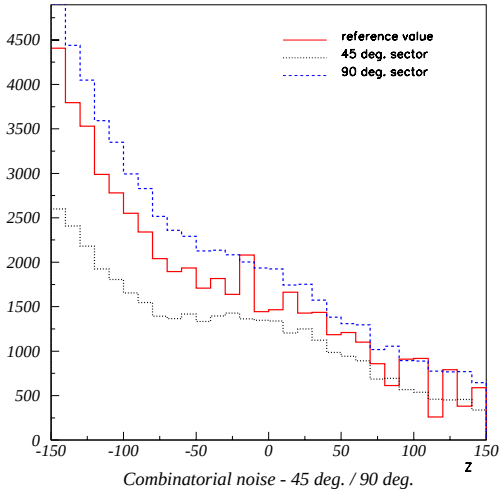

Figure 4: Combinatorial background combinations for a bin size of 5 mm for a sensor with the TDR-design (red/full-line), design 1-45° (black/dotted line) and design 1-90° (blue/dashed-line).

1-45° Design 1, and not combining 45° sectors to 90° sectors, but enhancing the capability of the Vertex Finder hardware to be able to cope with the increased number of channels..

1-90° Design 1, but combining 45° sectors to 90° sectors by OR-ing neighbouring sectors.

3.1 Pile-up Veto performance

In Fig. 4 the combinatorial background is shown for a fixed 5 mm bin size. Clearly the background is the lowest for the separate 45° sectors. This should have effect on finding the first and second interaction vertices. However, the effect is not that big.

In Fig. 5 the accepted values are shown for 1, 2 and more vertices for the three configurations for "all" and for "hard" minimum, bias events. For "all" the actual number of generated vertices is taken to qualify an event as a single or multiple vertex event. This includes diffraction and elastic scattering vertices. For "hard" events only vertices generated by a QCD process are counted, as they will be the main source of tracks so that the others can be neglected in comparison. The bin-sizes are as described in the thesis of Nikolai Zaitsev [3] [1]. For the events with just one vertex the accepted fraction goes down for the 90° sectors. Clearly, the increase in combinatorics degrades the performance slightly. For the events with multiple vertices the acceptance is lower; the difference between the acceptance of 1 and multiple events is worse.

The loss in acceptance due to the Pile-up Veto for 3 different physics samples is given in Table 3.1. Here the sample used for comparison is the offline accepted sample without trigger cuts. The loss is within errors the same for both the TDR and the 45° sector design.

[1] Bin size is 1 mm for -15≤z≤-10, 2 mm for -10≤z≤-5 cm, 3 mm for -5≤z≤4 cm and 5 mm for 4≤z≤15 cm.

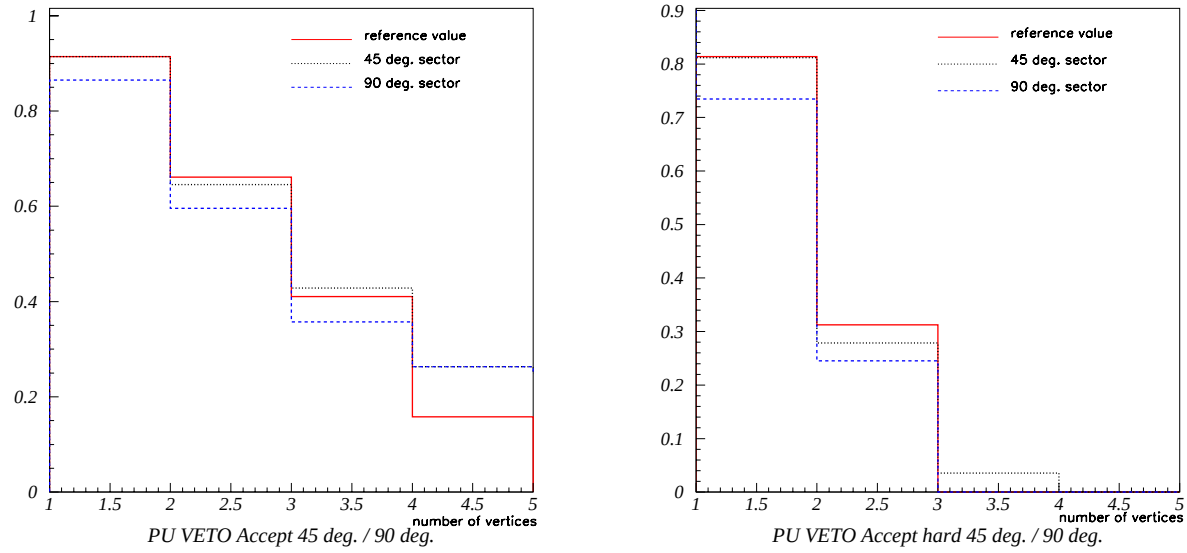

Figure 5: Pile-up Veto acceptance as function of the number of MC vertices in the event for all minimum bias (left) and hard minimum bias (right) events for a sensor with the TDR-design (red/full-line), design 1-45° (black/dotted line) and design 1-90° (blue/dashed-line).

Phys. Chann.	Cut on 2		Cut on 3	
	TDR	$1-45°$	TDR	$1-45°$
B$\rightarrow \pi\pi$	20±3	23±4	3±2	6±2
B$\rightarrow$D$_s$K	24±4	31±3	7±3	11±3
B$\rightarrow J/\psi\Phi$	22±5	28±5	3±2	5±2

Table 1: Loss of single events in 3 physics channels for the TDR design and for the separate 45° sector design for cuts on the second peak of 2 and 3, respectively.

3.2 Hardware consequences

The number of channels is depending on the detector configuration. In the non-combined case the total number of VETO channels is 1024. In case of combining 45° sectors the number becomes 760 for the TDR and 512 the 45° sector case. If one leaves out those channels that are not used in the correlation matrix one can omit an extra 10%. However, then e.g. calibration of the detector with halo muons is not possible anymore.

For the hybrid the consequence of combining the sectors at the detector level is, that just half of the number of Beetle chips is needed. That would make the hybrid much simpler. In case of combining at the Input Modules the number of optical links is about 90, otherwise just half of that. Fig. 6 schematically compares the different hardware implementations. Because we want to minimize losses in physics performance, we will pursue an implementation which will allow the use of all 1024 channels.

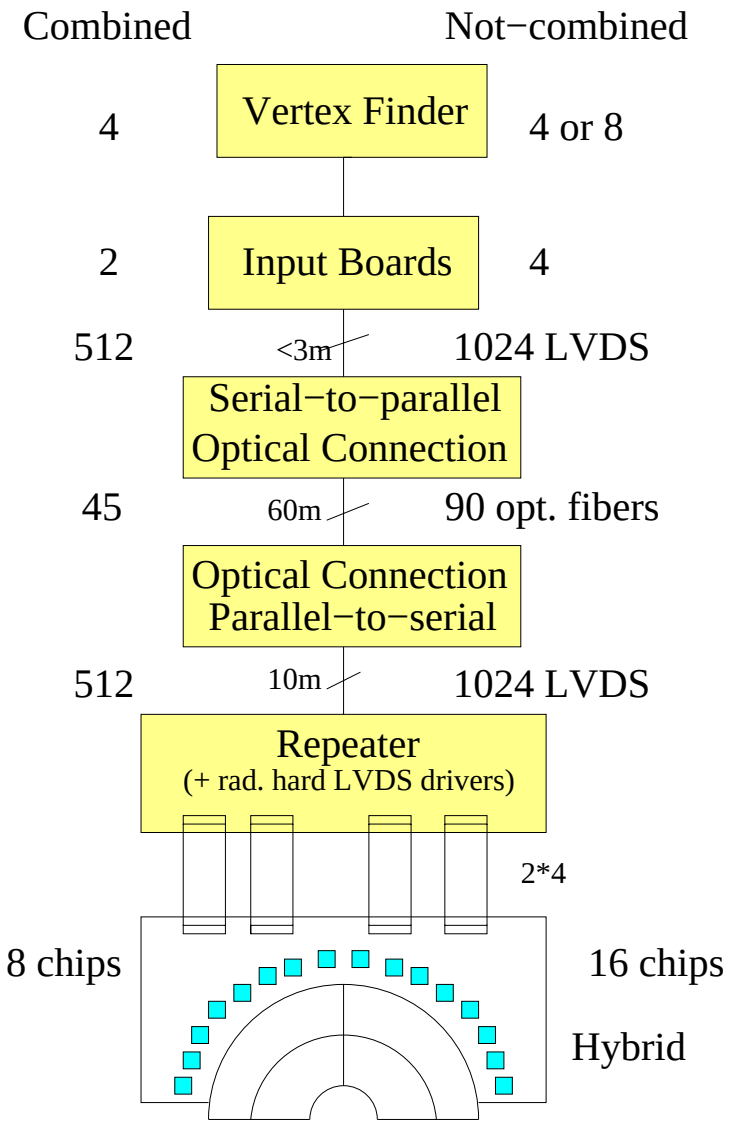

Figure 6: Pile-up Veto system with the number of connections and boards for a) combined 45° detector sectors (left) and b) not-combined sectors (right).

4 L1 tracking analysis

The change in R-sensor layout will affect both the tracks reconstruction in the VELO, and the extrapolation of VELO tracks to TT. These are discussed in the following two sub-sections.

4.1 L1 VELO tracking

To compare 90° and 45° geometries the L1 track reconstruction program has been slightly modified (for instance, number of sectors was increased etc.).

Here we present results of comparison of 2D and 3D tracking efficiency, primary vertex resolution and timing.

Table 2 shows tracking efficiencies for all designs. Here we split all tracks into subsets of tracks either of physical interest or important for analyzing the algorithm itself. A track

	2D tracking, %				3D tracking, %			
	TDR	45-1	45-2	45-3	TDR	45-1	45-2	45-3
Ref B Long	97.0	97.7	97.4	97.9	95.2	95.5	94.8	95.4
Ref Prim Long	98.9	99.1	98.6	99.1	97.8	98.0	97.7	98.0
Ref B	95.7	96.6	96.4	97.1	92.3	92.9	92.3	93.0
Ref Prim	97.8	98.7	98.3	98.4	95.2	95.7	95.4	95.6
Ref set	96.1	97.0	96.7	96.9	93.1	93.7	93.5	93.7
All set	92.2	93.6	93.4	93.6	87.4	88.3	88.2	88.3
Extra	77.6	81.1	81.1	81.5	66.2	68.5	68.4	68.3
Clone	5.7	4.5	4.6	4.5	5.3	4.5	4.7	4.6
Ghost	11.9	6.3	7.2	6.7	9.9	7.2	7.8	7.4

Table 2: Comparison of 2D and 3D tracking efficiency (in %) for different designs.

is considered as geometrically accepted (and thus included into performance analysis) if it crosses active areas in at least 3 VELO stations. These tracks form "All set" of tracks. The "Ref set" includes tracks with momentum larger than 1 GeV. Tracks with significant effects of multiple scattering form the "Extra set", i.e. "Extra" = "All" – "Ref". For primary and secondary vertices reconstruction we evaluate also reference primary tracks and daughter tracks from B decays ("Ref Prim" and "Ref B" in the table). To support track matching we calculate efficiency also for tracks having hits in downstream detectors ("Ref B Long" and "Ref Prim Long").

If at least 70% of the hits of a reconstructed track correspond to the same simulated track, the Monte-Carlo track is considered as found. If two (or more) reconstructed tracks correspond to the same MC track, only one track is used to associate with the MC track, but other tracks are called "Clone". If there is no 70%-correspondence found for a reconstructed track to a simulated track, such a reconstructed track is called "Ghost". In practice 70% correct hits is enough to provide good fitting parameters of reconstructed tracks.

One can see that the 45° geometry provides 0.5–1.0% higher efficiency for all reference sets of tracks. The most significant improvement is a twice lower ghost level in 2D tracking, directly resulting in better primary vertex resolution (see Table 3). A lower ghost level together with an almost 5% higher efficiency for extra tracks show that tracking can be done easier thus giving space for speeding up the most time consuming combinatorial part of the algorithm — 2D tracking.

	TDR	45-1	45-2	45-3
x	22.6	21.4	22.2	20.3
y	29.7	25.5	27.6	26.3
z	83.6	65.9	76.6	85.7

Table 3: The primary vertex resolution (in μm) for different designs.

The primary vertex resolution presented in Table 3 clearly shows better results for

45-1 design. The decrease of the z-resolution for other 45° designs can be explained by different strip pitch models, especially because the track fit uses 3 R hits.

	TDR	45-1	45-2	45-3	%
Input data	5.9	6.2	6.2	6.5	8.5
2D	7.2	5.3	5.5	5.9	7.1
getSpacePoint	53.7	50.4	50.2	52.8	67.9
3D	13.1	12.3	12.2	12.8	16.5

Table 4: Timing results (in msec) for different designs.

Timing results (Table 4) have been obtained running the algorithm on lxplus035 at CERN. There are 4 important parts in the current implementation of the L1 reconstruction algorithm:

1. **Input data** — transformation of input data from Gaudi format into internal structures.
2. **2D** — tracking in RZ–projection, including combinatorial track search (non-polynomial dependence on number of hits) and track competition (linear dependence on number of tracks).
3. **getSpacePoint** — call getSpacePoint function from the DeVelo library to obtain crossing point of R and ϕ strips.
4. **3D** — reconstruction of tracks in space using ϕ measurements.

One should mention that the L1 algorithm makes full reconstruction of all tracks (roughly 80 tracks per event in the test data sample) and thus is written in off-line style providing high efficiency for physical analysis and flexibility with respect to different detector geometries. Once both the detector geometry and the L1 algorithm are stable, the reconstruction algorithm will be investigated to speed it up. It is especially important for 2D tracking in its combinatorial part. It is also expected that only 5-10 tracks with large impact parameters will be selected for 3D reconstruction. The 3D part of the algorithm is not yet fixed also because of necessity to call an external function (at the time of the test — getSpacePoint) before searching for tracks in space.

4.2 VELO→TT reconstruction at L1

The quality of matching VELO and TT track segments is crucial for the momentum measurement at L1. Since the mean extrapolation distance is about two meters, the precise measurement of the track slope at last VELO hits is essential. In order to satisfy the execution time conditions at L1, a dedicated fast straight line fit to all VELO hits was developed. For each L1 3D track the $x_i, y_i, z_i, (i = 1, n)$ space points are constructed from (r, z) and (ϕ, z) cluster pairs of adjacent VELO sensors and the errors compatible with

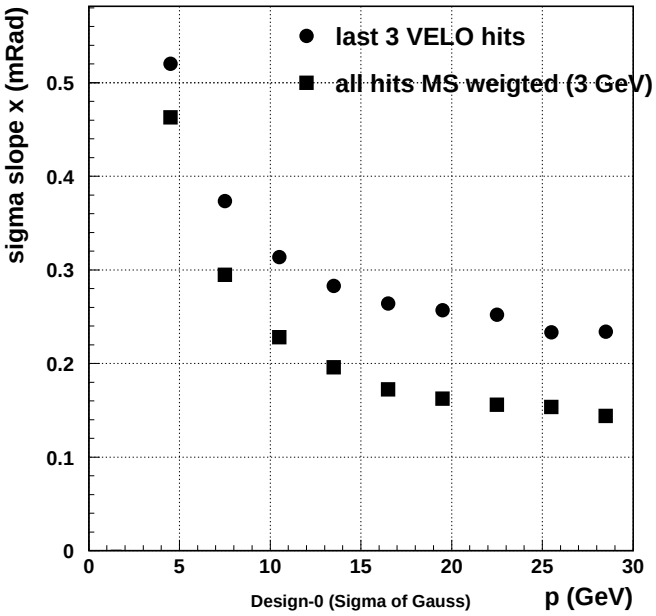

Figure 7: The comparison of the standard "last 3 hits" and the dedicated method for the slope determination at the last VELO hit for the extrapolation to TT.

the L1 resolution are assigned $\sigma_{x_i}^{L1}$ and $\sigma_{y_i}^{L1}$. Then these errors are modified according to a formula:

$$\sigma_{x_i,y_i} = \sqrt{(\sigma_{x_i,y_i}^{L1})^2 + (\sigma_i^{MS})^2} \tag{1}$$

where σ_i^{MS} takes into account the multiple scattering in consecutive downstream VELO stations. The scattering effect for 3 GeV particle was assumed since only the tracks with relatively high p_T are useful for extracting B events from the minimum bias background:

$$(\sigma_i^{MS})^2 = \sum_{k=i+1}^{n} (z_k - z_i)^2 * (\sigma_\theta^{MS})^2 \tag{2}$$

This way the error of the first points in VELO will contain the MS contributions coming from all downstream stations, thus having less weight in the line fit. On the contrary the last point at the VELO exit will contain only detector errors. This method makes use of all information contained in the VELO hits in an optimal way for the extrapolation to TT for the tracks with momenta above 3 GeV. The xz and yz projections are treated independently. The effect of such procedure is shown in Fig. 7. The track angular resolution for the whole range of momenta above 3 GeV improves with respect to the "last 3 hits" method used in the standard L1 VELO reconstruction where no momentum information is available.

In order to extract the difference coming from strip layouts in the four VELO designs studied, one has to reduce the influence of multiple scattering effects inside VELO sensors by looking at tracks with relatively high momentum. The angular resolutions of the x

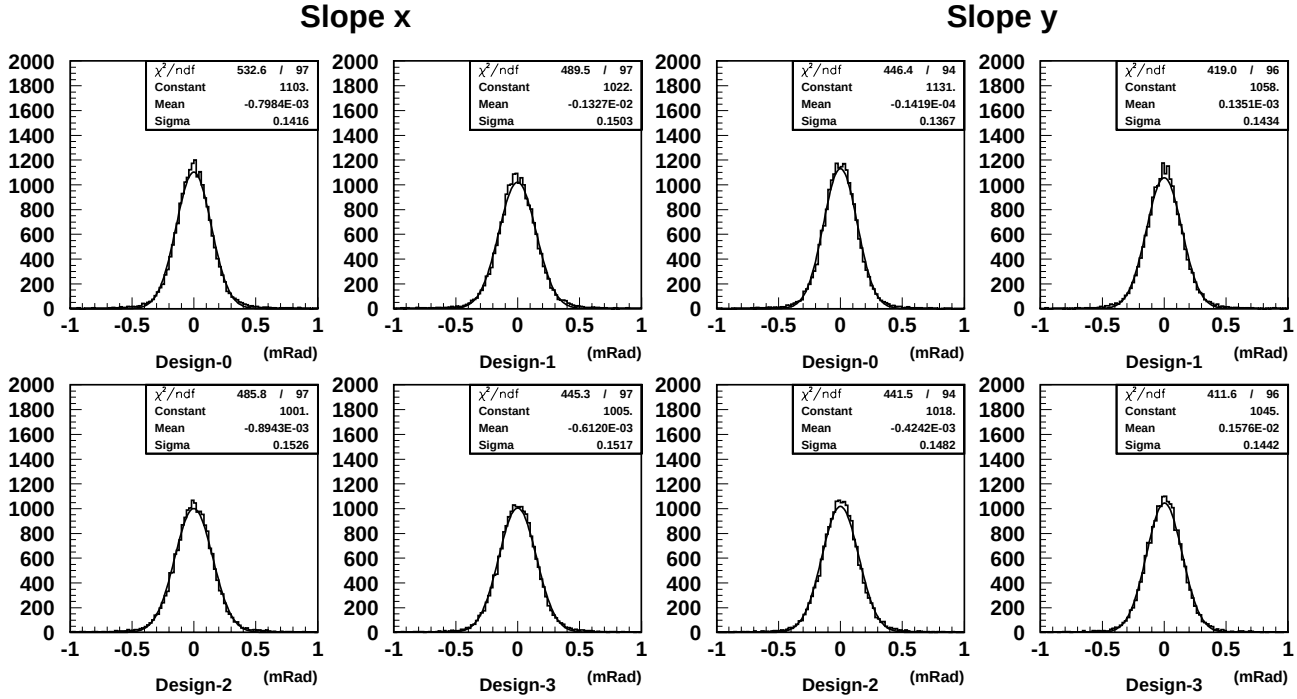

Figure 8: Angular resolutions obtained for the x and y slopes for the four VELO designs

and y track slopes measured for particles with momentum above 15 GeV are collected in Table 5 and the distributions are shown in Fig. 8. The resolutions were obtained by comparing the MC truth slopes constructed from last two GEANT hits in the VELO to the results of the dedicated straight line fit. All 45° designs (Design-1,-2 and -3) are similar and about 7% worse than the TDR design. The impact of this difference is small since momentum resolution is already at the level of 20% and dominated by multiple scattering in the material between VELO and TT.

The other parameters important for the L1 performance as the efficiency of track reconstruction, the rates of wrong TT matchings, p_T mistakes and VELO ghosts matched, are shown in Table 6. The rate of p_T mistakes is defined as the percentage of all tracks with $p_T^{MC} < 1$ GeV, $p_T > 1$ GeV and $p_T > 1.5 * p_T^{MC}$, where p_T^{MC} and p_T denote the true and reconstructed momenta respectively. The separation between signal and minimum bias events is very sensitive to the number of such false high p_T tracks which produce more incorrect positive decisions of L1 trigger. No significant difference of this parameter is seen among the four designs.

Taking into account all parameters from the two Tables 5 and 6, one can conclude that the TDR design is better than Designs-1,-2 and -3 in the angular resolution of the track at the VELO exit but is worse in the rate of VELO ghosts matched to TT. This difference has no significant effect on the overall performance of VELO-TT reconstruction and therefore the trigger performance is expected to be similar for all four designs.

5 Off-line tracking

The track reconstruction efficiency, ghost rate and track parameters of the off-line track reconstruction in the VELO have been compared between the four designs. While the reconstruction efficiency drops by 0.4-1.0%, depending on the track selection, the ghost

Design	σ_x^{slope} [mRad]	σ_y^{slope} [mRad]
TDR	0.142 ± 0.001	0.137 ± 0.001
Design-1	0.150 ± 0.001	0.143 ± 0.001
Design-2	0.153 ± 0.001	0.148 ± 0.001
Design-3	0.152 ± 0.001	0.144 ± 0.001

Table 5: The x and y angular resolutions obtained by the dedicated straight line fit to all VELO hits for $p > 15$ GeV tracks for the four VELO designs.

Design	Efficiency. ($p > 5$ GeV tracks) [%]	Wrong matchings [%]	p_T assignment mistakes [%]	Matched VELO ghosts [%]
TDR	84.6 ± 0.4	2.39 ± 0.07	6.3 ± 0.1	1.60 ± 0.06
Design-1	84.3 ± 0.4	2.37 ± 0.07	6.3 ± 0.1	1.36 ± 0.06
Design-2	83.9 ± 0.4	2.35 ± 0.07	6.5 ± 0.1	1.38 ± 0.06
Design-3	83.8 ± 0.4	2.30 ± 0.07	6.3 ± 0.1	1.32 ± 0.06

Table 6: The performance parameters of VELO-TT reconstruction for the four VELO designs.

rate drops from 5.7% for the TDR design to 4.1-4.3% for designs 1-3. It is very probable that with some retuning to the new 45° design the efficiency could be equalized, at the cost of a equivalent ghost rate. The comparison of the errors of the track parameters shows that the TDR design and design-1 are essentially the same, while designs 2 and 3 are a few % worse in both the position and slope. The main difference lies in the execution time of the algorithm, which is improved by nearly 50% with the new designs.

6 Impact parameter resolution

The effect of the design changes on the track impact parameter resolution has been studied. A small degradation in performance is anticipated for the new designs due to the increased strip pitches required to change from 90° to 45° outer sectors.

The track impact parameter was projected on to the plane containing the beam axis and the first GEANT hit point in the VELO. The reconstructed impact parameter was calculated with respect to the true origin of the simulated particle. ${K^0}_s$ and secondary interactions were suppressed by requiring the true origin of the particle to be < 3mm from the beam axis.

The impact parameter resolution is dependent on the multiple scattering of the track (approximately $\propto 1/p$) and the track extrapolation distance ($\propto p/p_t$), where p and p_t are the track momentum and the momentum projected in plane transverse to the beam direction. Hence, the impact parameter is best analysed as a function of $1/p_t$.

The impact parameter distributions obtained were fitted in bins of $\log(1/p_t)$. Single

Gaussians were fitted to each bin and acceptable χ^2/dof fits obtained. The sigma of each Gaussian, the resolution, for the four designs studied is shown in the top plot of Fig. 9. The error bars indicate the statistical errors for uncorrelated samples, the true uncertainty is smaller than this as the same events were used for all studies. The variation of resolution as a function of $1/p_t$ is clearly visible. The plot covers the range $0.14 < p_t < 4.5$ GeV/c.

However, the difference between the designs is not clearly visible. The lower part of Fig. 9 shows the relative performance of the three new designs with respect to the TDR design. Horizontal line fits have been performed in the momentum range 4.5 GeV/c to 0.5 GeV/c. Design 1 shows an impact parameter degradation of $5.3 \pm 0.8\%$, design 2 of $4.9 \pm 0.8\%$ and design 3 of $4.1 \pm 0.8\%$.

From these results there appears to be a tendency, although the difference is small, for better performance from the new designs in which the first measured point on the track is more accurately determined: design 3 with all tracks obtaining a first point in the 40 μm pitch region performs better than design 1 in which the pitch increases over this region. The importance of the first measured point on the track is further reinforced in Fig. 10. Here, the study has been performed again with several variants on design 1 with different pitch ranges. In the lower plot the relative performance of the models are shown with respect to the standard design 1 (pitch range of 40 to 103 μm). Performing straight line fits, as above, shows an improvement of $8.5 \pm 0.7\%$ with the 20 to 157 μm design, $4.5 \pm 0.7\%$ with the 30 to 125 μm design and a degradation of $4.9 \pm 0.7\%$ for a 50 to 86 μm design. However, fabrication constraints will not permit a significant reduction from 40 μm for the inner pitch, and charge loss may be risked if the outer pitch is significantly increased.

The upper plot of Fig. 10 also shows the extreme effect of reducing the number of strips in the VELO R sensors by a factor of two and imposing a constant pitch of 133 μm.

This analysis was performed using forward and matched tracks with a modified Brunel v14r0 on 5000 $B \to \pi\pi$ events with minimum bias spillover events included.

7 Conclusion

The move to a 45° design was originally motivated by the improvement observed in the L1 VELO tracking. For this algorithm the 45° designs show an improvement in both the clone and ghost rates, while the execution time of the algorithm is reduced, and the efficiency to find tracks is at least similar if not improved. The off-line VELO tracking shows a similar behaviour, the main improvement being observed in the execution time. In addition the new layout equalises the load capacitance for the FE-amplifiers, resulting in a more homogeneous response function, which will facilitate finding an optimum timing. The 90° regions on the detector gave the lowest S/N, and are expected to improve by up to 40% for the worst regions when moving to a 45° design.

Keeping the same number of channels per sensor has the adverse effect that the strip pitch has to be increased. The influence of this increased pitch has been studied for the Pile-up Veto, the extrapolation from VELO to TT and the impact parameter resolution.

For the Pile-up Veto a deterioration in the performance is observed when the implementation maintains 90° sectors to perform the algorithm. However, on the one hand the loss in LHCb physics capability will not noticeably be affected by this deterioration, while the performance can be recovered by changing to an implementation exploiting the 45° sectors. This 45° implementation will be pursued.

Linking VELO tracks to TT shows a deterioration in the angular resolution of the VELO tracks due to the increased pitch at larger radii, however with retuning the efficiency can be recovered, while the ghost rate is reduced due to the smaller ghost rate in the L1 VELO tracks.

The off-line impact parameter resolution shows a $\sim 5\%$ deterioration by moving to 45° designs, with a slight P_t dependence. This deterioration can be avoided by going to a 45° design where the pitch at small radii is reduced from 40 μm to 30 μm or even smaller, at the expense of increasing the pitch at larger radii from 103 μm to 125 μm or even larger. However, the final physics performance will be dominated by the efficiency of the sensors, and reducing the pitch significantly below 40 μm introduces fabrication risks, while increasing the pitch at larger radii risks charge loss for thin sensors and deteriorates the downstream extrapolation precision for linking to other tracking stations.

Hence, in conclusion, the preferred option is design 45-1, which contains a pitch range which has been used already in pre-production sensors and satisfies the physics requirements.

References

[1] LHCb Vertex Locator Technical Design Report, CERN/LHCC 2001-011.

[2] LHCb-2000-025. Search for pixel clusters in the VELO silicon strip detector by Smith, H ; 06 Sep 2000

[3] Study of the LHCb Pile-up trigger and $B_S \to J/\psi\phi$ decay / Zaitsev, N Y; CERN , 27 Oct 2000 . - 130 p . - CERN-THESIS-2000-043

[4] Detector Geometry - Vertex Locator test-beam software desription, C. Parkes, LHCb-2000-096.

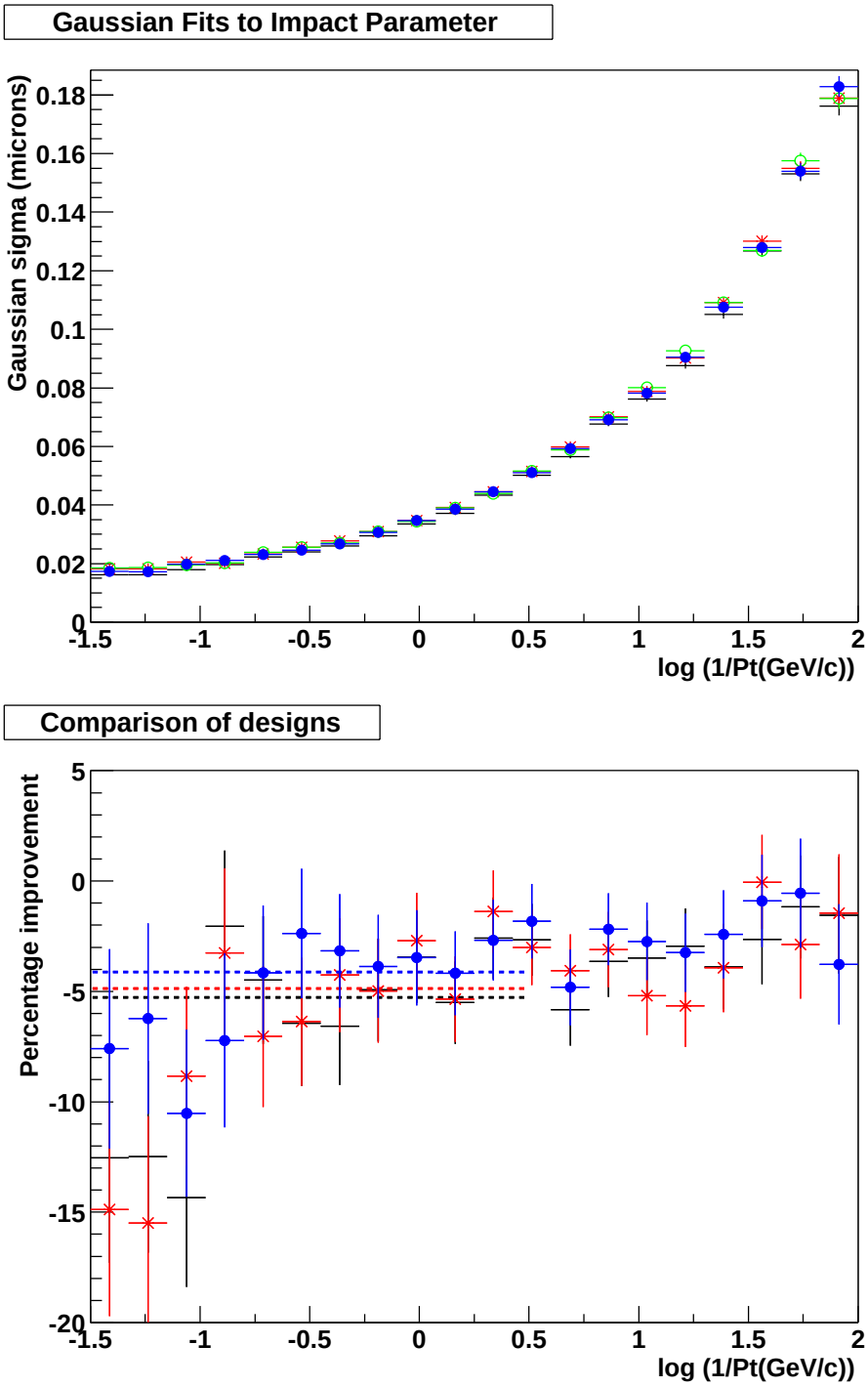

Figure 9: A comparison of the impact parameter resolution (see text) of the 4 VELO designs under study. The resolution is plotted in bins dependent on the transverse momentum of the tracks. In the upper plot design 0 is shown as the black points, design 1 is shown as red asterisks, design 2 as green open circles and design 3 as blue filled circles. The lower plot shows the same data re-plotted to show the performance of the new designs relative to design 0. The black points show the relative performance of design 1, the red asterisks design 2 and the blue filled circles design 3.

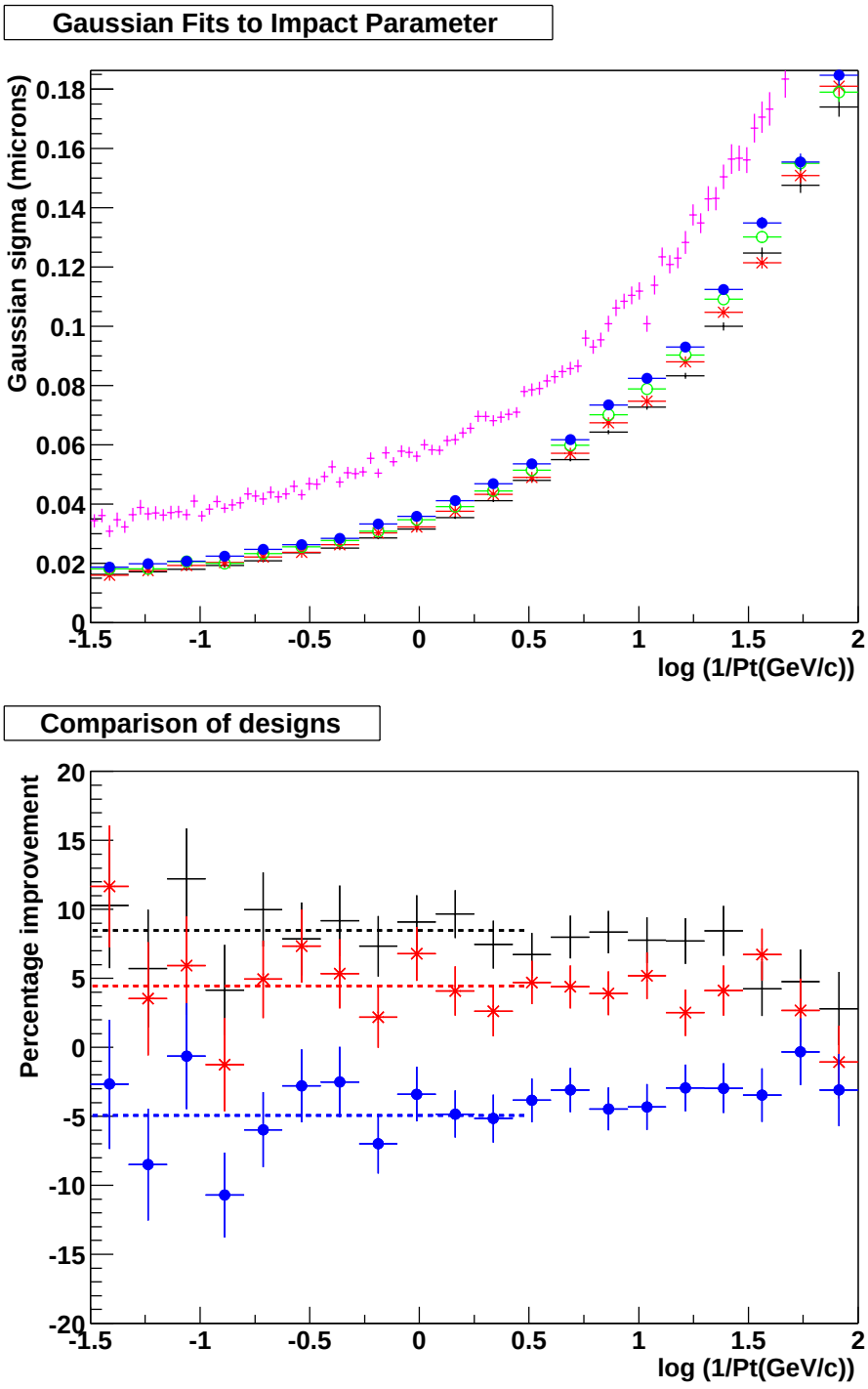

Figure 10: A comparison of the impact parameter resolution of variants on VELO design 1 (see text). The resolution is plotted in bins dependent on the transverse momentum of the tracks. In the upper plot a design in which the pitch range is 20 to 157 μm is shown as the black points, the 30 to 125 μm pitch design is shown as red asterisks, the 40 to 103 μm standard design 1 as green open circles and a 50 to 86 μm variant as blue filled circles. The lower plot shows the same data re-plotted to show the performance of theses variant designs relative to the 40 to 103 μm design. The black points show the relative performance of the 20 to 157 μm pitch range, the red asterisks the 30 to 125 μm design and the blue filled circles the design with pitches ranging from 50 to 86 μm. Magenta points have also been added to the upper plot showing the large degradation in performance if the number of strips in the VELO R sensors was halved.